Author Manuscript

Author Manuscript

Author Manuscript

Author Manuscript

HHS Public Access

Author manuscript

Toxicol Appl Pharmacol. Author manuscript; available in PMC 2020 December 18.

Published in final edited form as:

Toxicol Appl Pharmacol. 2020 December 01; 408: 115280. doi:10.1016/j.taap.2020.115280.

Biological effects of inhaled hydraulic fracturing sand dust. V. Pulmonary inflammatory, cytotoxic and oxidant effects

Tina M. Sager*, **Jenny R. Roberts**, **Christina M. Umbright**, **Mark Barger**, **Michael L. Kashon**, **Jeffrey S. Fedan**, **Pius Joseph**

Health Effects Laboratory Division, National Institute for Occupational Safety and Health, 1095 Willowdale Road, Morgantown, WV 26505, United States of America

Abstract

The pulmonary inflammatory response to inhalation exposure to a fracking sand dust (FSD 8) was investigated in a rat model. Adult male Sprague-Dawley rats were exposed by whole-body inhalation to air or an aerosol of a FSD, i.e., FSD 8, at concentrations of 10 or 30 mg/m^3, 6 h/d for 4 d. The control and FSD 8-exposed rats were euthanized at post-exposure time intervals of 1, 7 or 27 d and pulmonary inflammatory, cytotoxic and oxidant responses were determined. Deposition of FSD 8 particles was detected in the lungs of all the FSD 8-exposed rats. Analysis of bronchoalveolar lavage parameters of toxicity, oxidant generation, and inflammation did not reveal any significant persistent pulmonary toxicity in the FSD 8-exposed rats. Similarly, the lung histology of the FSD 8-exposed rats showed only minimal changes in influx of macrophages following the exposure. Determination of global gene expression profiles detected statistically significant differential expressions of only six and five genes in the 10 mg/m^3, 1-d post-exposure, and the 30 mg/m^3, 7-d post-exposure FSD 8 groups, respectively. Taken together, data obtained from the present study demonstrated that FSD 8 inhalation exposure resulted in no statistically significant toxicity or gene expression changes in the lungs of the rats. In the absence of any information about its potential toxicity, a comprehensive rat animal model study (see Fedan, J.S., *Toxicol Appl Pharmacol*. 000, 000–000, 2020) has been designed to investigate the bioactivities of several FSDs in comparison to MIN-U-SIL® 5, a respirable α-quartz reference dust used in previous animal models of silicosis, in several organ systems.

*Corresponding author at: Toxicology and Molecular Biology Branch, National Institute for Occupational Safety and Health, 1000 Frederick Lane, Morgantown, WV 26508, United States of America., sst2@cdc.gov (T.M. Sager).

CRediT authorship contribution statement

Tina M. Sager: Validation, Formal analysis, Investigation, Writing - original draft, Writing - review & editing. **Jenny R. Roberts:** Validation, Formal analysis, Investigation, Resources, Visualization, Writing - original draft, Writing - review & editing. **Christina M. Umbright:** Software, Validation, Formal analysis. **Mark Barger:** Validation. **Michael L. Kashon:** Formal analysis. **Jeffrey S. Fedan:** Conceptualization, Resources, Methodology, Writing - original draft, Writing - review & editing. **Pius Joseph:** Resources, Methodology, Writing - original draft.

Publisher's Disclaimer: Disclaimer

Publisher's Disclaimer: The findings and conclusions in this report are those of the authors and do not necessarily represent the official position of the National Institute for Occupational Safety and Health, Centers for Disease Control and Prevention. Mention of any company or product does not constitute endorsement by the National Institute for Occupational Safety and Health (NIOSH), Centers for Disease Control and Prevention (CDC).

Declaration of competing interest

The authors declare that they have no conflicts of interest in relation to this publication.

Author Manuscript Author Manuscript Author Manuscript Author Manuscript

Keywords

Fracking sand dust; Pulmonary toxicity; Gene expression; Inflammation; Lung; Rats

1. Introduction

Hydraulic fracturing ("fracking") is a process that involves the injection of a large volume of pressurized fluid containing proppants to fracture shale and facilitate the flow of natural gas and/or oil into the well bore for extraction. A significant increase in fracking, resulting in corresponding increases in oil and natural gas production in the U.S., has been reported in recent years (USGAO, 2012). For example, in 2013, hydraulic fracturing accounted for 30% of the natural gas production in the U.S. (Newell and Iler, 2013). Similarly, hydraulic fracturing has been attributed as one of the major reasons for the increase in domestic oil production in the U.S., which is currently at levels exceeding those of its import (USEIA, 2019).

Sand, commonly referred as fracking sand, is a proppant used in hydraulic fracturing. The amount of sand used as proppant in hydraulic fracturing depends on the complexity of the well and, in some cases, this may be in excess of one million tons of sand per well. Mechanical handling of the sand to prepare it as a proppant involves hauling large quantities of sand in trucks to the drilling site, moving it along transfer belts, and pneumatically filling and operating sand movers. Such processes typically result in the generation of air-born dust containing fine fracking sand particles, i.e., fracking sand dust (FSD).

Based on the results of a field study conducted by NIOSH investigators (Esswein et al., 2013), significant quantities of crystalline silica were detected in the FSD collected from hydraulic fracturing sites in the U.S. These investigators analyzed 111 personal breathing zone samples collected from 11 hydraulic fracturing sites spread over five states in the U.S. Crystalline silica was present in all the samples. In addition, the amount of crystalline silica detected in many of the samples collected and analyzed exceeded the Occupational Safety and Health Administration (OSHA) Permissible Exposure Limit (PEL) of 50 $\mu g/m^3$ (Szymendera, 2016) and the National Institute for Occupational Safety and Health (NIOSH) Recommended Exposure Limit (REL) of 50 $\mu g/m^3$ (NIOSH, 1994). This raises serious concerns about the potential for exposure to crystalline silica among workers engaged in hydraulic fracturing, which could lead to adverse health effects.

Significant occupational exposure to crystalline silica has been reported among workers engaged mining (Peters et al., 2017), sand blasting (Radnoff et al., 2014), foundry work (Kuo et al., 2018), construction (Bello et al., 2019) and other industrial sectors. Inhalation is the main route for occupational exposure to dust containing crystalline silica, and most of the serious health effects associated with occupational exposure to crystalline silica are thought to be those affecting the lungs. An excessive tuberculosis burden has been reported among individuals who are exposed to crystalline silica (Hnizdo and Murray, 1998). The International Agency for Research on Cancer (IARC), based on the findings of animal and human studies, have classified crystalline silica as a human carcinogen (IARC, 1997). A serious lung disease associated with exposure to crystalline silica is silicosis, an irreversible

Author Manuscript Author Manuscript Author Manuscript Author Manuscript

and potentially fatal lung disease (NIOSH, 2002), accounting for approximately one hundred deaths per year in the U.S. alone (NIOSH, 2017). Prevention of silicosis by avoiding or reducing occupational exposure to crystalline silica is a priority for NIOSH (NIOSH, 2002) and OSHA (Szymendera, 2016).

Despite the finding that workers engaged in hydraulic fracturing are at risk of exposure to crystalline silica that is present in the FSD (Esswein et al., 2013), whether their exposure to the dust results in adverse health effects is not known. Currently, the pulmonary inflammatory response potentially resulting from whole-body inhalation exposure of rats to FSD was determined and the results are presented in this communication. This report is the fifth in a series of tandem papers in which the potential toxicity of FSD (FSD 8) has been comprehensively investigated. The first paper in the series (Fedan, 2020) describes the overall approach to the investigation in the context of current knowledge about silica toxicity and research gaps. Other studies in this series have examined the effects of FSD 8 on lung ventilatory and non-ventilatory functions, inflammatory mechanisms, cardiovascular, and immune systems, brain and blood (Russ et al., 2020; Anderson et al., 2020; Krajnak et al., 2020; Sriram et al., 2020) and cytotoxicity (Olgun et al., 2020), and have been summarized (Investigative Team, 2020).

2. Methods

2.1. Animals

Adult male Sprague-Dawley rats [H1a: (SD) CVF], weighing approximately 200–250 g, were obtained from Hilltop Lab Animals, Inc. (Scottdale, PA) for this study. All animals were free of viral pathogens, parasites, mycoplasm, *Heliobacter*, and cilia-associated respiratory bacillus. The rats, upon arrival, were acclimated to animal facility conditions for about a week prior to their use in the study. Once acclimated, the rats were housed, in pairs, in ventilated micro-isolator units supplied with HEPA-filtered laminar flow air (Thoren Caging Systems; Hazleton, PA), with 7090 Sani Chip and 7070C Diamond Dry combination (both from Harlan, now Envigo; Indianapolis, IN) for bedding, and provided tap water and 2918 irradiated Teklad Global 18% rodent diet (Harlan, now Envigo; Indianapolis, IN) ad libitum. The rats were housed under controlled light cycle (12 h light/12 h dark) and temperature (22–25 °C) conditions.

All procedures involving the rats were conducted in the AAALAC International-accredited animal facility at NIOSH following protocols (14-JF-R-004, 16-JF-R-018 v8, 17–013 v5, 19–010 v4, and 19–015 v2) that were approved by the CDC-Morgantown Institutional Animal Care and Use Committee and were in compliance with the Public Health Service Policy on Humane Care and Use of Laboratory Animals and the NIH Guide for the Care and Use of Laboratory Animals.

2.2. Physical and chemical characterization of FSD 8 particles

The FSD 8 was obtained from a well pad during fracking operations. Its physical and chemical properties are described in Fedan et al. (2020).

Author Manuscript Author Manuscript Author Manuscript Author Manuscript

2.3. Generation of FSD 8 aerosol

An aerosol containing FSD 8 was generated as described in detail in Russ et al. (2020).

2.4. Inhalation exposure of rats to FSD 8

Rats were exposed by whole-body inhalation to an aerosol containing FSD 8 at concentrations of 10 or 30 mg/m^3, 6 h/d for 4 d. Control animals were exposed to filtered air and were otherwise handled similarly. During their 6-h inhalation exposure to air or FSD 8, the rats were not provided with food or water. The exposure chamber and conditions during the inhalation exposure of the rats were as described in Fedan et al. (2020).

2.5. Euthanasia of rats and collection of biospecimens

At post-exposure time intervals of 1, 7 and 27 d, the control and FSD 8-exposed rats were euthanized by overdose of sodium pentobarbital containing euthanasia solution (100–300 mg/kg, i.p.; Fatal Plus; Vortec Pharmaceuticals, Dearborn, MI) followed by exsanguination. Rats were euthanized and samples collected following a 90-d post-exposure time interval in the case of the rats exposed to the dust at the higher concentration of 30 mg/m^3. The trachea was then cannulated, the chest cavity was opened, the right bronchi were clamped off, and bronchoalveolar lavage (BAL) was performed on the left lung (Sellamuthu et al., 2011).

The acellular fraction of the first lavage was obtained by filling the left lung with 3 ml/100 g body weight of cold phosphate-buffered saline (PBS), massaging for 30 s, withdrawing, and repeating the process once. This concentrated aliquot was withdrawn, retained on ice, kept separately, and was designated as the first fraction of BAL fluid (BALF). The subsequent aliquots were 4 ml in volume, instilled once with light massaging, withdrawn, and combined until a 24 ml-volume was obtained. For each animal, both lavage fractions were centrifuged (10 min, 570 ×*g*, 4 °C), the cell pellets were combined and re-suspended in 1 ml of PBS, and the acellular fluid from the first fraction was retained for further analysis.

Following euthanasia, right lung lobes (cardiac and diaphragmatic) were removed and were pressure-fixed in 10% neutral buffered formalin by airway pressure fixation under 30 cm water pressure to total lung capacity for 15 min. Lung volumes were assessed by weight of water displacement. Once the fixation process was complete, the lung lobes were paraffin embedded, sectioned, and stained with hematoxylin and eosin (H&E). The apical lobe from the right lung of the rats was cut into pieces and stored in RNAlater (Invitrogen; Carlsbad, CA).

2.6. Analysis of BALF lactate dehydrogenase (LDH) activity and cytokines levels

LDH activity in the BALF of the rats exposed to filtered air or FSD 8 was measured to evaluate cytotoxicity as an index of lung injury. LDH activity was determined as described previously (Sellamuthu et al., 2011). A battery of 27 proteins was also evaluated in BALF samples using a multi-plex assay for cytokine array (Eve Technologies Corporation; Calgary, Canada.).

Author Manuscript Author Manuscript Author Manuscript Author Manuscript

2.7. Cell differentials: alveolar macrophages (AMs), neutrophils, lymphocytes and eosinophils

The total numbers of BAL cells collected from rats exposed to air or FSD 8 were counted using a Coulter Multisizer II (Coulter Electronics; Hialeah, FL). Cell differentials were performed to determine the total number of AM, neutrophils, lymphocytes, and eosinophils. Briefly, 10^5 cells from each rat were spun down onto slides with a Cytospin 3 centrifuge (Shandon Life Sciences International; Cheshire, England) and labeled with Leukostat stain (Fisher Scientific; Pittsburgh, PA) to differentiate cell types. Two hundred cells per slide were counted, and the percentages of AMs, neutrophils, lymphocytes and eosinophils were multiplied by the total number of lavaged cells to calculate the total number of each cell type.

2.8. FSD 8 particle detection in AMs

The cytospin slides prepared from all the control and FSD 8-exposed rats were observed under a light microscope for particles representing inhaled FSD 8.

2.9. Oxidant generation by lung phagocytes

To estimate lung phagocyte oxidant production, luminol-dependent chemiluminescence (CL) was performed on BAL cells as a measure of the light generated by the production of reactive oxygen species (ROS) by AM and PMN using a Berthold LB953 luminometer (Wallace Inc.; Gaithersburg, MD), as described previously (Antonini et al., 1994). Baseline oxidant production by the cells was measured in the absence of a stimulant. Luminol (Sigma-Aldrich; St. Louis, MO) was used to enhance detection of the light, and 0.2 mg/ml of unopsonized zymosan (Sigma-Aldrich) or phorbol 12-myristate 13-acetate 3 (PMA; 10 μM; Sigma-Aldrich) was added to the assay immediately prior to the measurement of CL to activate the cells. PMA, a soluble stimulant of total BAL phagocytes (AM and PMN), was added to the assay immediately prior to CL measurement to determine the contribution of both AM and PMN to the overall production of ROS in the lungs. Additionally, because rat neutrophils do not respond to unopsonized zymosan, the zymosan-stimulated CL produced is from AMs. Measurement of CL (for both PMA and zymosan-stimulated calls) was recorded for 15 min at 37 °C, and the integral of counts per minute (cpm) per 10^6 cells vs. time was calculated. CL was calculated as the cpm of the stimulated cells minus the cpm of the corresponding resting cells, and the value was normalized to total number of BAL cells for PMA-stimulated CL and total number of AM in the BAL for zymosan-stimulated CL.

2.10. Lung histopathology

For histopathological analysis, H&*E*-stained sections of right lung tissue from each animal were evaluated for parameters of injury and inflammation. Slides were quantitatively analyzed by a certified veterinary pathologist at Charles River Laboratories (Frederick, MD). The pathologist was blinded to the treatment groups. Indices of inflammation, injury, and structural changes were scored on scale of 0 to 5, where 0 = no observed effect, 1 = minimal response, 2 = mild response, 4 = moderate response, and 5 = severe response.

Author Manuscript Author Manuscript Author Manuscript Author Manuscript

2.11. RNA isolation from lung samples

Total RNA, free of contaminating genomic DNA and proteins, was isolated from a piece of the lung tissue using RNeasy Mini Kit (Qiagen, Inc.; Valencia, CA) following the procedure provided by the manufacturer. The integrity and purity of the RNA samples isolated were determined using the Agilent 2100 Bioanalyzer (Agilent Technologies; Palo Alto, CA). Total RNA was quantified by UV-Vis spectrophotometry. Only RNA samples exhibiting an RNA Integrity Number (RIN) ≥8.0 were used in the gene expression studies.

2.12. Determination of lung gene expression profile

One microgram total RNA/sample was used to create sequencing libraries using the Illumina TruSeq® Stranded Total RNA Library Prep (Illumina, Inc.; San Diego, CA) following the protocol provided by the manufacturer. Stated briefly, following depletion of ribosomal RNA (rRNA), the RNA samples were purified, fragmented (68 °C for 5 min), and primed for cDNA synthesis. The denatured and cleaved RNA fragments were purified using a bead cleanup procedure and reverse transcribed into first strand cDNA using reverse transcriptase and random primers. While synthesizing the double stranded cDNA, dUPT was incorporated in place of dTTP followed by the addition of a single 'A' nucleotide to the 3 prime ends to facilitate proper adapter ligation to each sample. Indexing adapters provided in the library preparation kit were ligated to the ends of the ds cDNA. After adapter ligation, the samples were PCR amplified (12 cycles) to enrich the DNA fragments containing the adapter molecules and to enhance the amount of DNA in the library using a Veriti™ 96 Well Thermal Cycler (Applied Biosystems; Foster City, CA). The PCR amplified the cDNA library samples were quantified using a dsDNA HS Assay Kit (Invitrogen by ThermoFisher Scientific) and Qubit 3.0 Fluorometer (Invitrogen by ThermoFisher Scientific; Waltham, MA). Average fragment size and fragment distribution of the cDNA library samples were then assessed using an Agilent 2100 Bioanalyzer (Agilent Technologies; Santa Clara, CA) with High Sensitivity DNA Reagents (Agilent Technologies). The validated samples were sequenced on an Illumina HiSeq 2500 (Illumina, Inc.).

Individual sample libraries were provided to the Centers for Disease Control and Prevention Genome Sequencing Laboratory (GSL; Atlanta, GA) for 2 × 50 (low dose) or 2 × 75 (high dose) base pair paired-end sequencing using the Illumina HiSeq 2500 (Illumina Inc.) in rapid run mode using HiSeq Rapid Cluster Kit v2 (Illumina Inc.) and HiSeq Rapid SBS Kit v2 (Illumina, Inc.).

After the library sequences were de-multiplexed by the GSL, the quality of each sample library was assessed with respect to the number of reads per sample, mean quality score, and FASTQC parameters (Andrews, 2010). Reads were then processed using Trimmomatic/0.35 with the options PE, ILLUMINACLIP:TruSeq2-PE.fa:2:30:10 LEADING:3 TRAILING:3 SLIDINGWINDOW:4:15 MINLEN:36 (low dose) or MIN-LEN:60 (high dose) to remove any remaining adapter sequence, low quality reads, low quality read ends, and sequences shorter than 36 (low dose) or 60 (high dose) bases in length (Bolger et al., 2014). Sequence quality was then reevaluated via FASTQC (Andrews, 2010). All sequences that passed the trimming and quality control with both reads in a pair present were aligned to the *Rattus norvegicus* Rnor 6.0 genome from NCBI downloaded July 31, 2015 using HiSat2/2.1.0

Author Manuscript Author Manuscript Author Manuscript Author Manuscript

(Kim et al., 2015) and Bowtie2/2.2.9 (Langmead and Salzberg, 2012). Raw gene counts were assigned using Samtools/1.8 (Li et al., 2009), Python/2.7.3 and HTSeq/0.6.1 (Simon et al., 2014). Using edge R, raw counts were converted to counts per million (CPM) and log-CPM and then normalized (R Core Team, 2018). Finally, differentially expressed genes were calculated using limma (Law et al., 2016). Differentially expressed genes were those genes with a fold change greater than 1.5-fold between the controls and the FSD 8-exposed rats and an adjusted P value less than 0.05.

The next generation sequencing data presented in this manuscript have been deposited in the Gene Expression Omnibus (GEO) Database (http://www.ncbi.nlm.nih.gov/geo) and are accessible through GEO accession number GSE148255.

2.13. Statistical analysis

Results for all BAL were expressed as mean fold change from control. A one-way analysis of variance (ANOVA) was performed between all treatment groups at each time point. Significant differences among groups were determined using the Student-Newman-Keuls post hoc test. Data were analyzed using SigmaPlot for Windows Version 14.0 (Systat Software, Inc.; Ekrath, Germany). For all analyses, significance was set at $P < 0.05$. Statistical significance of the pulmonary toxicity parameters measured in the BALF were assessed using a one-way ANOVA for variance at each time point with the Student Newman Keuls (SNK) post hoc test for significance. Because data from histopathology studies were inherently categorical, a nonparametric analysis of variance was performed using SAS, Inc. (Cary, NC) statistical programs using the Wilcoxon rank sum test.

3. Results

3.1. Animals

No difference in physical activity, food or water consumption, and body weight gain was noticed in any of the FSD 8-exposed rats, compared with the air-exposed control rats (not shown and Fedan et al., 2020).

3.2. Detection of FSD 8 particles in alveolar macrophages

Black/brown particles representing inhaled FSD 8 particles were detected in the AMs of lung samples collected from all the FSD 8-exposed rats at all the post-exposure time intervals analyzed (Fig. 1). More AMs contained FSD 8 particles in the 30 mg/m^3 groups compared to those obtained from the 10 mg/m^3 groups. The highest number of FSD 8 particles in the AMs was detected at 1-d post-exposure and a steady decline in the number of particles was noticed at later post-exposure intervals. No FSD 8 particles were detected in the lungs of the control, air-exposed rats (data not presented).

3.3. BAL parameters of pulmonary toxicity

Compared with the time-matched controls, no statistically significant differences in the BALF LDH activity were detected in the lungs from both groups of the FSD 8-exposed rats at any of the post-exposure time intervals (Fig. 2). The number of total BAL cells in any of the FSD 8-exposed rats, compared with the corresponding controls also were not affected by

Author Manuscript Author Manuscript Author Manuscript Author Manuscript

FSD 8 exposure (Fig. 3). AMs accounted for greater than 97% of all cells in all groups. However, a statistically significant increase in the number of PMNs in the BAL was detected in the FSD 8-exposed rats at 7 d at 10 mg/m^3 and at 1 d at 30 mg/m^3 (Fig. 4). However, although the increases were statistically significant, they only accounted for 1.5 and 0.8% of the total cells, respectively at those time points.

Cytokines levels in the BALF, overall, were not affected significantly by any FSD exposure compared with the corresponding controls (Tables 1 and 2).

There were no differences in the PMA- or zymosan-stimulated generation of chemiluminescence by the phagocytes present in the BALF of any of the FSD 8-exposed rats at any of the post-exposure time intervals compared with the controls (Fig. 5).

3.4. Lung histology

Following exposure to the low dose of fracking sand, there was a statistically significant increase in AMs at day 1 and 7 scored as 1 (minimal) on scale of 0 to 5. The presence of fracking sand was also scored as positive for 1 and 7 d post-exposure. By day 27, there were no changes in the lung associated with injury or inflammation. There was also a statistically significant increase in AMs 1 d following exposure to the high dose of FSD 8 scored as 1 (minimal) on a scale of 0 to 5 (not shown). There were no statistically significant changes in parameters of lung injury or inflammation at any other time point. Particles were scored as present in AMs up to d 27 d post-exposure.

3.5. Gene expression profiles in lungs

No statistically significant changes in the global gene expression profiles were detected in the lungs of the majority of the FSD 8-exposed rats. Statistically significant differential expression of six genes was detected in the 10 mg/m^3 FSD 8-exposed rats at the 1-d post-exposure time interval (Table 3). Among the six differentially expressed genes (SDEGs), three were over-expressed in the FSD 8-exposed lungs while the expressions of the remaining three genes were down-regulated, compared with the air-exposed controls. The gene *Dbp* exhibited the highest differential expression of 5.42-fold in this group of FSD 8-exposed rat lungs, compared with the controls. Among the rats exposed to the 30 mg/m^3 FSD 8, five SDEGs were detected 7-d post-exposure (Table 4). The expressions of all five SDEGs in this group of rats were downregulated compared with the controls. The most significant change in expression (10.56-fold) was noticed in the case of LOC103691832 gene. In general, the fold changes in expressions of the genes were higher in the 30 mg/m^3 group (−2.33- to 10.56-fold) compared with the 10 mg/m^3 group (1.56 to −3.08-fold). None of the SDEGs detected in the 10 mg/m^3 group was found significantly differentially expressed in the 30 mg/m^3 group of rats and vice versa.

4. Discussion

Occupational inhalation exposure to dust containing crystalline silica is a serious concern, primarily because of the various adverse health effects that are known to be associated with the exposure. Lungs, in addition to being the primary route for occupational exposure to crystalline silica, are conventionally regarded as being the primary targets for the resulting

Author Manuscript Author Manuscript Author Manuscript Author Manuscript

toxicity and adverse health effects. Extensive studies have been conducted in the past, by employing animal models, investigating the pulmonary toxicity of crystalline silica, as well as the mechanisms underlying the toxicity.

Previous studies conducted by NIOSH investigators have demonstrated that whole-body inhalation exposure of rats to crystalline silica (MIN-U-SIL 5®) resulted in the onset and progression of pulmonary toxicity, including inflammatory and pre-silicotic responses (Castranova et al., 2002; Porter et al., 2004; Sellamuthu et al., 2011, 2012, 2013, 2017). In the series of studies reported by Sellamuthu et al., adult male Fischer rats were exposed by whole-body inhalation exposure to air or an aerosol containing MIN-U-SIL 5® (15 mg/m^3, 6 h/d for 5 d). Compared with the controls, the rats exposed to MIN-U-SIL 5® exhibited significant alterations in a number of measures: BALF LDH activity and cytokine levels, counts of BAL AMs and PMNs, lung histology, and lung gene expression profile (Sellamuthu et al., 2011, 2012, 2013, 2017). Based on their findings, these authors concluded that whole-body inhalation exposure of rats to crystalline silica resulted in the immediate induction of pulmonary toxicity, which steadily progressed during the post-exposure time intervals that ranged from 1 day to 44 weeks.

Hydraulic fracturing, despite its contribution to the increase in oil and natural gas production in the U.S. in recent years, has raised environmental (USGAO, 2012) and public health (Vidic et al., 2013) concerns. As well, safety and the health of workers engaged amidst exposure to FSDs containing high levels of crystalline silica during hydraulic fracturing is a serious concern mainly because of the potential for lung diseases. Analysis of 111 personal breathing zone samples collected from 11 geographically different locations in the U.S. showed the universal presence of crystalline silica in FSD (Esswein et al., 2013). In some cases, the amount of crystalline silica present in the FSD samples was up to 20-fold higher than the NIOSH REL or OSHA PEL. This has raised questions regarding the potential health effects among workers employed in hydraulic fracturing, since excessive exposure to crystalline silica is known to result in potentially fatal diseases including cancer (IARC, 1997) and silicosis (NIOSH, 2002).

The FSD 8 sample used in the current study was comprised of >95% crystalline silica (Fedan et al., this issue). Inhaled silica particles entering the lungs are phagocytized predominantly by the AMs for their detoxification and elimination. As expected, inhalation exposure of rats to the respirable FSD 8 particles (Fedan et al., 2020) resulted in alveolar deposition of these particles. Pathological examination indicated that the particles had been engulfed by macrophages (Fig. 1). In the absence of efficient detoxification and elimination, the inhaled particles could give rise to lung toxicity. A significant elevation in BALF LDH activity, a general indicator of cytotoxicity, has been associated with pulmonary toxicity induced by inhaled MIN-U-SIL 5® in rat lungs (Porter et al., 2004; Sellamuthu et al., 2011). In contrast, the observation that comparable levels of BALF LDH activity were detected in the lungs of the air-breathing control and FSD 8-exposed rats (Fig. 2) suggests the absence of any significant pulmonary cytotoxicity induced by FSD 8 exposure in the rats under the conditions employed in the present study. This was further substantiated by the absence of any significant histological changes in both dose cohorts of the FSD 8-exposed rats at all post-exposure time intervals analyzed.

Author Manuscript Author Manuscript Author Manuscript Author Manuscript

Exposure to crystalline silica has been shown to result in the induction of oxidative stress, which has also been shown to be a component of the mechanism of crystalline silica toxicity (Castranova et al., 2002; Porter et al., 2004). The observation that there was no difference in the lung phagocytes-mediated generation of chemiluminescence detected in the air- and FSD 8-exposed rats (Fig. 5) may suggest that FSD 8 exposure, under the conditions employed in the study, did not result in the induction of oxidative stress in the rat lungs, in the manner reported previously for MIN-U-SIL 5®.

Induction of inflammation in the lung is a hallmark of crystalline silica exposure (Castranova, 2004). An increase in the number of infiltrating PMNs in the lungs and elevations in BALF cytokine levels have been reported in response to exposure of rats to MIN-U-SIL 5® crystalline silica (Sellamuthu et al., 2011). A significant increase in BAL PMN number in response to FSD 8 inhalation exposure was observed only in two out of the seven post-exposure groups analyzed in this study, and it resolved by day 27 following inhalation of either dose (Fig. 3). Similarly, the levels of many of the cytokines from FSD 8-exposed rats were comparable to those of the controls (Tables 1 and 2). These results, therefore, indicate that the FSD 8 exposure in the rats, under the exposure conditions employed in this study, did not result in an appreciable inflammatory response.

Previously, Sellamuthu et al. (2011, 2012, 2013, 2017) detected significant changes in hundreds of genes in the lungs of rats in response to their inhalation exposure to Min-U-SIL 5®. Global gene expression profiling in the lungs of the FSD 8-exposed rats in the current study, in contrast, did not detect any significant changes in the gene expression profile in the majority of the post-exposure groups. This, in agreement with the results of the inflammatory marker measurements (Figs. 2–4 and Tables 1 and 2), also suggests that FSD 8 exposure in the rats, under the conditions employed in the present study, did not result in significant pulmonary responses.

It is noteworthy that the inhalation exposure of rats to FSD 8 did not result in a persistent pulmonary response. Furthermore, an expected linearity in the dose-response and time-response relationships was not observed, and the reason(s) for this requires future investigation. The reason(s) for the lack of a pulmonary response in the rats exposed to FSD 8 in the current study needs further investigation. The route of exposure, parameters employed to assess lung toxicity, and the post-exposure time intervals selected to determine the toxicity in the current study were comparable to those employed by Sellamuthu et al. (2011, 2012, 2013, 2017), who reported significant changes in all those toxicity parameters, demonstrating the induction of pulmonary toxicity in Min-U-SIL 5®-exposed rats. The present study was conducted in Sprague-Dawley rats, whereas many of the previous NIOSH studies investigated pulmonary responses to Min-U-SIL 5® toxicity in Fischer rats (Castranova et al., 2002; Porter et al., 2004; Sellamuthu et al., 2011, 2012, 2013, 2017). It is unlikely that the strain of the rats employed accounts for the appreciable differences between Min-U-SIL 5® and FSD 8 toxicity detected since crystalline silica-induced pulmonary toxicity has been detected in Fischer (Porter et al., 2002, Porter et al., 2004; Sellamuthu et al., 2011, 2012, 2013, 2017), Sprague-Dawley (Farris et al., 2017), and Lewis (Langley et al., 2010) strains of rats. It is, however, possible that the association of other minerals on the surfaces of the particles of FSD 8 employed in the current study (Fedan et al., 2020)

Author Manuscript Author Manuscript Author Manuscript Author Manuscript

prevented, through masking, cellular interactions that would trigger an inflammatory response. It is of interest to determine whether FSDs collected from other hydraulic fracturing sites in the U.S. would, in this rat inhalation model, have a similar toxicity profile as the dust examined in the present study.

Acknowledgements

Funding was provided by the National Institute for Occupational Safety and Health, Project Number 7927ZLDC.

References

Anderson SE, Shane H, Long C, Marrocco A, Lukomska E, Roberts JR, Marshall N, Fedan JS, 2020 Biological effects of inhaled hydraulic fracturing sand dust. VIII. Immunotoxicity. Toxicol. Appl. Pharmacol (Manuscript submitted to this journal as a tandem paper to accompany this manuscript).

Andrews S, 2010 FastQC: A Quality Control Tool for High Throughput Sequence Data http://www.bioinformatics.babraham.ac.uk/projects/fastqc.

Antonini JM, Van Dyke K, Ye Z, DiMatteo M, Reasor MJ, 1994 Introduction of luminol-dependent chemiluminescence as a method to study silica inflammation in the tissue and phagocytic cells of rat lung. Environ. Health Perspect 102 (Suppl. 10), 37–42.

Bello A, Mugford C, Murray A, Shepherd S, Woskie SR, 2019 Characterization of occupational exposures to respirable silica and dust in demolition, crushing, and chipping activities. Ann. Work Expo. Health 63, 34–44. [PubMed: 30379992]

Bolger AM, Lohse M, Usadel B, 2014 Trimmomatic: A flexible trimmer for Illumina sequence data. Bioinformatics 30, 2114–2120. [PubMed: 24695404]

Castranova V, 2004 Signaling pathways controlling the production of inflammatory mediators in response to crystalline silica exposure: role of reactive oxygen/nitrogen species. Free Radic. Biol. Med 37, 916–925. [PubMed: 15336307]

Castranova V, Porter D, Millecchia L, Ma JY, Hubbs AF, Teass A, 2002 Effect of inhaled crystalline silica in a rat model: time course of pulmonary reactions. Mol. Cell. Biochem 234–235, 177–184.

Esswein EJ, Breitenstein M, Snawder J, Kiefer M, Sieber WK, 2013 Occupational exposures to respirable crystalline silica during hydraulic fracturing. J. Occup. Environ. Hyg 10, 347–356. [PubMed: 23679563]

Farris BY, Antonini JM, Fedan JS, Mercer RR, Roach KA, Chen BT, Schwegler-Berry D, Kashon ML, Barger MW, Roberts JR, 2017 Pulmonary toxicity following acute coexposures to diesel particulate matter and alpha-quartz crystalline silica in the Sprague-Dawley rat. Inhal. Toxicol 29, 322–339. [PubMed: 28967277]

Fedan JS, 2020 Biological effects of inhaled hydraulic fracturing sand dust. I. Scope of the investigation. Toxicol. Appl. Pharmacol (Manuscript submitted to this journal as a tandem paper to accompany this manuscript).

Fedan JS, Hubbs AF, Barger M, Schwegler-Berry D, Friend S, Leonard SS, Thompson JA, Jackson MC, Snawder JE, C M, Dozier AK, Coyle J, Kashon ML, Park J−H, McKinney W, Roberts JR, 2020 Biological effects of inhaled hydraulic fracturing sand dust. II. Inhalation exposure system, particle characterization, and effects following intratracheal instillation. Toxicol. Appl. Pharmacol (Manuscript submitted to this journal as a tandem paper to accompany this manuscript).

Hnizdo E, Murray J, 1998 Risk of pulmonary tuberculosis relative to silicosis and exposure to silica dust in South African gold miners. Occup. Environ. Med 55, 496–502. [PubMed: 9816385]

International Agency for Research on Cancer (IARC), 1997 Silica, some silicates, coal dust and paramild fibrils. IARC Monogr. Eval. Carcinog. Risks Humans 68, 10475.

Investigative Team, 2020 Biological effects of inhaled hydraulic fracturing sand dust. IX. Summary and significance. Toxicol. Appl. Pharmacol (Manuscript submitted to this journal as a tandem paper to accompany this manuscript).

Kim D, Langmead B, Salzberg SL, 2015 HISAT: a fast spliced aligner with low memory requirements. Nat. Methods 12, 357–360. [PubMed: 25751142]

Author Manuscript Author Manuscript Author Manuscript Author Manuscript

Krajnak K, Russ KA, McKinney W, Waugh S, Zheng W, Kan H, Kashon ML, Johnson C, Cumpston J, Fedan JS, 2020 Biological effects of inhaled hydraulic fracturing sand dust. IV. Exposure to fracking sand dust results in changes in factors associated with cardiovascular dysfunction. Toxicol. Appl. Pharmacol (Manuscript submitted to this journal as a tandem paper to accompany this manuscript).

Kuo CT, Chiu FF, Bao BY, Chang TY, 2018 Determination and prediction of respirable dust and crystalline-free silica in the taiwanese foundry industry. Int. J. Environ. Res. Public Health 15 (10).

Langley RJ, Mishra NC, Pena-Philippides JC, Hutt JA, Sopori ML, 2010 Granuloma formation induced by low-dose chronic silica inhalation is associated with an anti-apoptotic response in Lewis rats. J. Toxicol. Environ. Health A 73, 669–683. [PubMed: 20391111]

Langmead B, Salzberg S, 2012 Fast gapped-read alignment with Bowtie 2. Nat. Methods 9, 357–359. [PubMed: 22388286]

Law CW, Alhamdoosh M, Su S, Smyth GK, Ritchie ME, 2016 RNA-seq analysis is easy as 1-2-3 with limma, Glimma and edgeR [version 2; referees;3 approved] F1000Research 5, 1408.

Li H, Handsaker B, Wysoker A, Fennell T, Ruan J, Homer N, Marth G, Abecasis G, Durbin R, 1000 Genome project data processing subgroup, 2009 The sequence alignment/map format and SAMtools. Bioinformatics 25, 2078–2079. [PubMed: 19505943]

National Institute for Occupational Safety and Health (NIOSH), 2002 Hazard review: Health Effects of Occupational Exposures to Respirable Silica. US Department of Helath and Human Services (NIOSH) Publication No. 2002–129. http://www.cdc.gov/niosh/docs/2002-129/02-129a.html.

Newell R, Iler S, 2013 The global energy outlook In: Kalicki JH, Goldwyn DL (Eds.), Energy and Security Strategies of a World in Transition. D.C Johns Hopkins University Press, Washington, pp. 25–68.

NIOSH, 1994 Pocket Guide to Chemical Hazards Found at: https://www.cdc.gov/niosh/npg.html.

NIOSH, 2017 Work-Related Lung Disease Surveillance System (eWoRLD) 2017–893 U.S. Department of Health and Human Services, Centers for Disease Control and Prevention, National Institute for Occupational Safety and Health, Respiratory Health Division, Morgantown, WV Available at: https://wwwn.cdc.gov/eworld/Data/893.

Olgun NS, Morris AM, Stefaniak AB, Bowers LN, Knepp AK, Duling MG, Mercer RR, Kashon ML, Fedan JS, Leonard SS, 2020 Biological effects of inhaled hydraulic fracturing sand dust. III. Cytotoxicity and pro-inflammatory responses in cultured murine macrophage cells. Toxicol. Appl. Pharmacol (Manuscript submitted to this journal as a tandem paper to accompany this manuscript).

Peters S, Vermeulen R, Fritschi L, Musk AB, Reid A, de Klerk N, 2017 Trends in exposure to respirable crystalline silica (1986–2014) in Australian mining. Am. J. Ind. Med 60, 673–678. [PubMed: 28692194]

Porter Dale W., Ye Jianping, Ma Jane, Barger Mark, Robinson Victor A., Ramsey Dawn, McLaurin Jeff, Khan Amir, Landsittel Douglas, Teass Alexander, Castranova Vincent, 2002 TIME COURSE OF PULMONARY RESPONSE OF RATS TO INHALATION OF CRYSTALLINE SILICA: NF-kappa B ACTIVATION, INFLAMMATION, CYTOKINE PRODUCTION, AND DAMAGE. Inhalat. Toxicol 14 (4), 349–367.

Porter DW, Hubbs AF, Mercer R, Robinson VA, Ramsey D, McLaurin J, Khan A, Battelli L, Brumbaugh K, Teass A, Castranova V, 2004 Progression of lung inflammation and damage in rats after cessation of silica inhalation. Toxicol. Sci 79, 370–380. [PubMed: 15056817]

R Core Team, 2018 R: A language and environment for statistical Computing R Foundation for Statistical Computing, Vienna, Austria URL. http://www.R-project.org/.

Radnoff D, Todor MS, Beach J, 2014 Occupational exposure to crystalline silica at Alberta work sites. J. Occup. Environ. Hyg 11, 557–570. [PubMed: 24479465]

Russ KA, Thompson JA, Reynolds JS, Mercer RR, Porter DW, McKinney W, Dey RD, Barger M, Cumpston J, Batchelor TP, Kashon ML, Kodali V, Sriram K, Fedan JS, 2020 Biological effects of inhaled hydraulic fracturing sand dust. IV. Pulmonary effects. Toxicol. Appl. Pharmacol (Manuscript submitted to this journal as a tandem paper to accompany this manuscript).

Sellamuthu R, Umbright C, Roberts JR, Chapman R, Young SH, Richardson D, Leonard H, McKinney W, Chen B, Frazer D, Li S, Kashon M, Joseph P, 2011 Blood gene expression profiling detects silica exposure and toxicity. Toxicol. Sci 122, 253–264. [PubMed: 21602193]

Author Manuscript Author Manuscript Author Manuscript Author Manuscript

Sellamuthu R, Umbright C, Roberts JR, Chapman R, Young SH, Richardson D, Cumpston J, McKinney W, Chen BT, Frazer D, Li S, Kashon M, Joseph P, 2012 Transcriptomics analysis of lungs and peripheral blood of crystalline silica-exposed rats. Inhal. Toxicol 24, 570–579. [PubMed: 22861000]

Sellamuthu R, Umbright C, Roberts JR, Cumpston A, McKinney W, Chen BT, Frazer D, Li S, Kashon M, Joseph P, 2013 Molecular insights into the progression of crystalline silica-induced pulmonary toxicity in rats. J. Appl. Toxicol 33, 301–312. [PubMed: 22431001]

Sellamuthu R, Umbright C, Roberts JR, Young SH, Richardson D, McKinney W, Chen BT, Li S, Kashon M, Joseph P, 2017 Molecular mechanisms of pulmonary response progression in crystalline silica exposed rats. Inhal. Toxicol 29, 53–64. [PubMed: 28317464]

Simon A, Pyl PT, Huber W, 2014 HTSeq - A Python framework to work with high-throughput sequencing data. Bioinformatics 31 (2), 166–169. [PubMed: 25260700]

Szymendera SD, 2016 Respirable crystalline silica in the workplace: new occupational safety and health administration (OSHA) standards. Congr. Res. Serv 7–5700.

United States Energy Information Administration (USEIA), 2019 US Crude Oil Production Contributes to GLOBAL OIL PRICE STABILITY in 2013 Available at. http://www.eia.gov/todayinenergy/detail.cmf?id=14531.

United States Government Accountability Office (USGAO), 2012 Oil and Gas Inforamtion on Shale Resources, Development, and Environmental and Public Health Risks Report to Congressional Requestors by Rusco F, Kehr C, Carroll L et al., (GAO-12–732).

Vidic RD, Brantley SL, Vandenbossche JM, Yoxtheimer D, Abad JD, 2013 Impact of shale gas development on regional water quality. Science 340, 1235009. [PubMed: 23687049]

Author Manuscript Author Manuscript Author Manuscript Author Manuscript

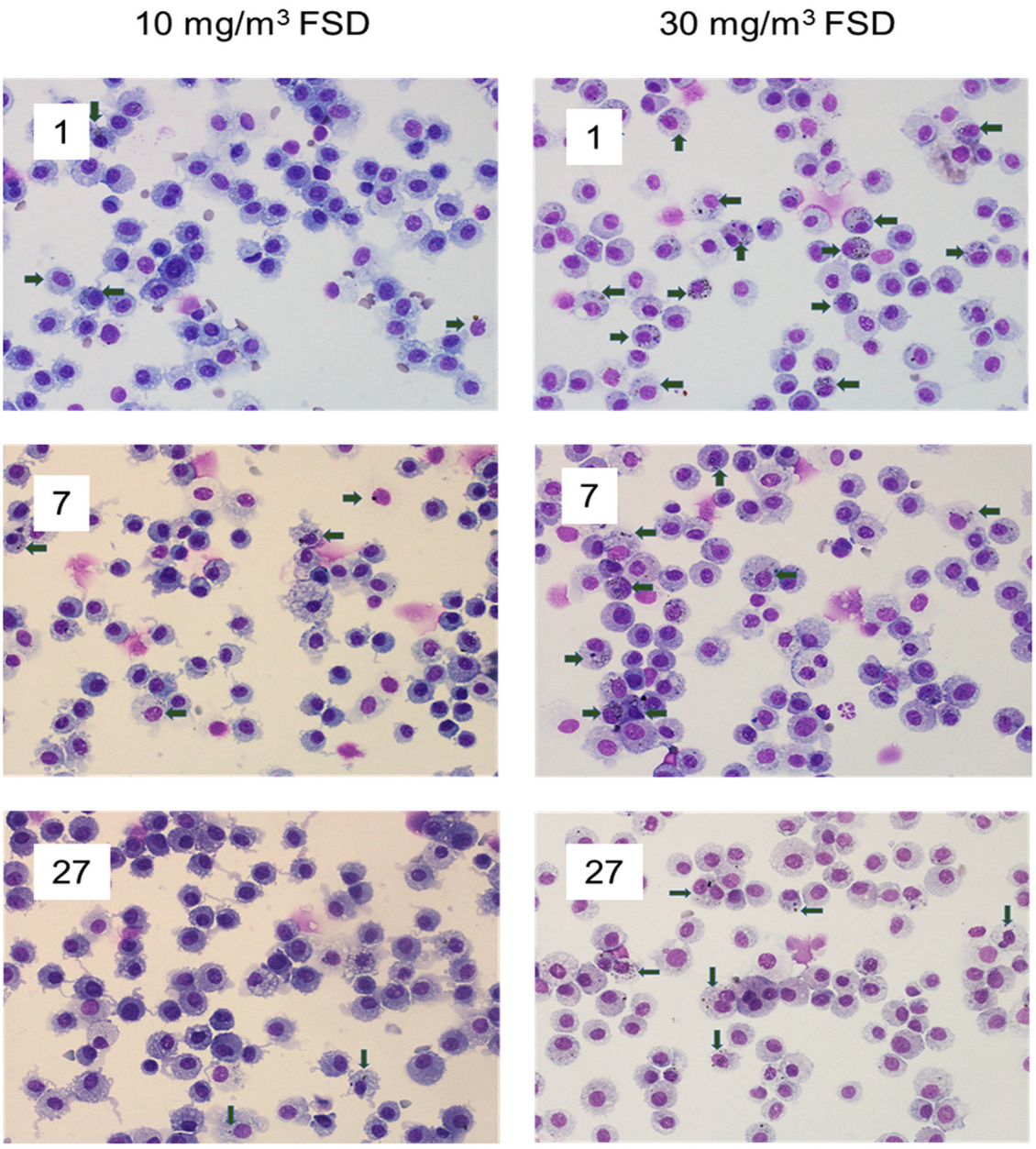

Fig. 1.

FSD 8 particles in alveolar macrophages following inhalation of 10 or 30 mg/m^3. (FSD 8 is abbreviated as FSD in the figures.) AMs obtained from rats at 1, 7 and 27 d post-exposure were observed under a light microscope to detect FSD 8 particles. The cells were stained with H&E.

Author Manuscript Author Manuscript Author Manuscript Author Manuscript

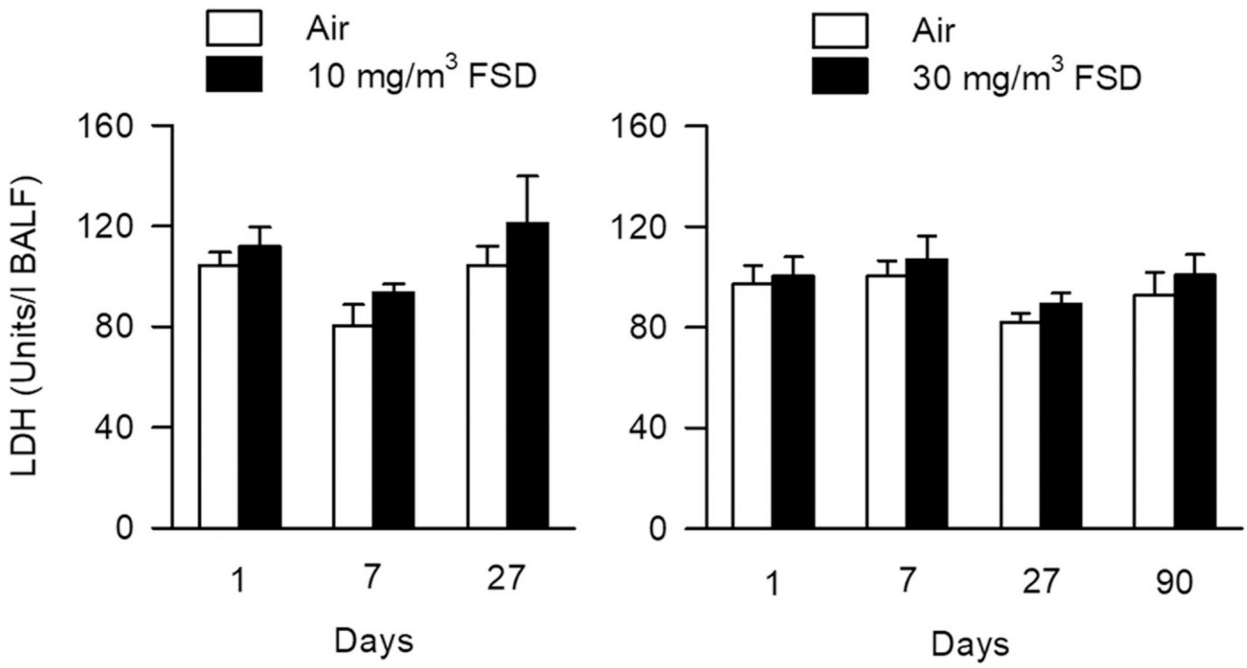

Fig. 2.

BALF LDH activity in rat lung. Rats were exposed to FSD 8 at 10 or 30 mg/m^3. BALF LDH was determined as described in the text at post exposure intervals as indicated in the figures following the exposure.

Author Manuscript Author Manuscript Author Manuscript Author Manuscript

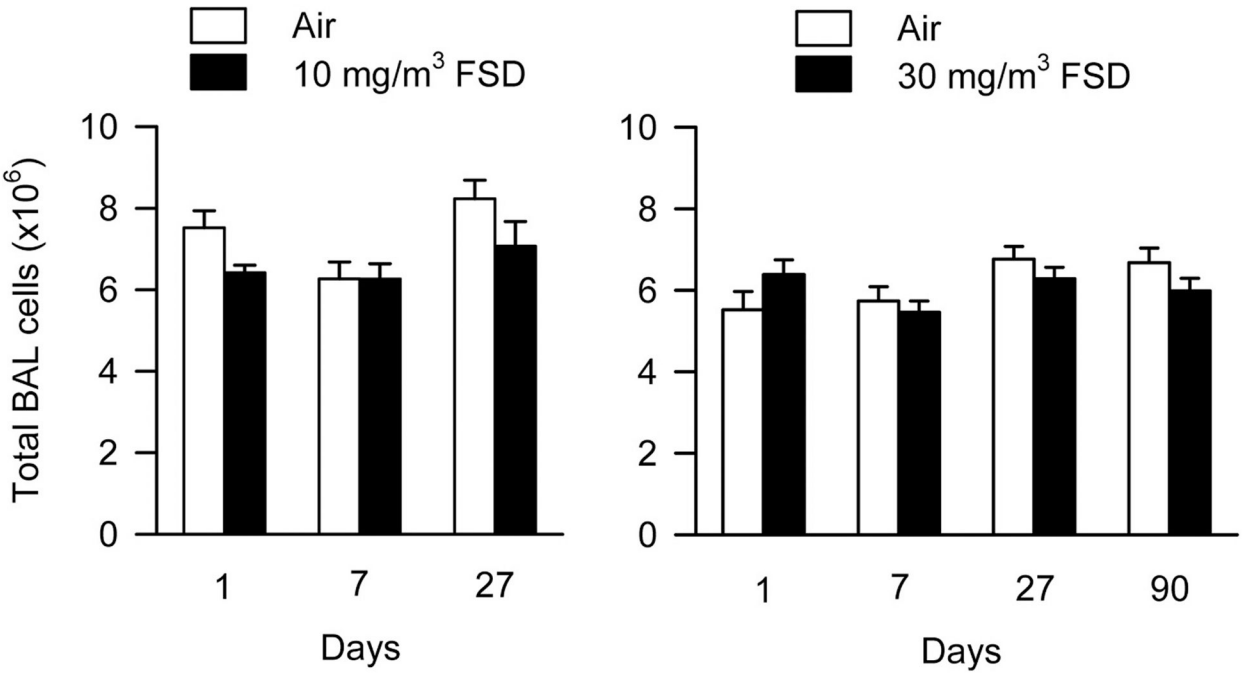

Fig. 3.

BAL cells in rat lungs. Rats were exposed to FSD 8 at 10 or 30 mg/m^3. The number of total cells in the BAL was determined at the post-exposure time intervals indicated in the figures as described in the text. The data represents the total number of cells obtained from rats at the indicated post-exposure time intervals following the exposure. AMs accounted for >97% of all cells in all groups.

Author Manuscript Author Manuscript Author Manuscript Author Manuscript

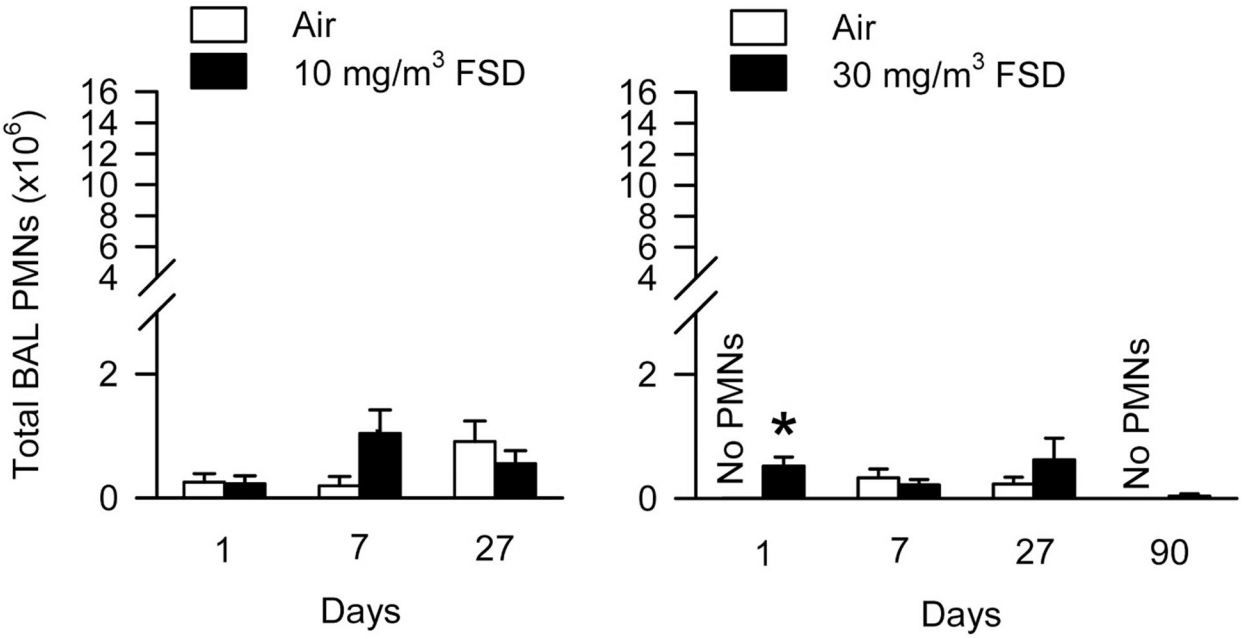

Fig. 4.

BAL PMNS in rat lungs. Rats were exposed to FSD 8 at 10 or 30 mg/m^3. The number of PMNs in the BAL was determined as described in the text. The data represents the total number of cells PMNs obtained from rats at the post-exposure time intervals as indicated in the figure following the exposure.

Author Manuscript Author Manuscript Author Manuscript Author Manuscript

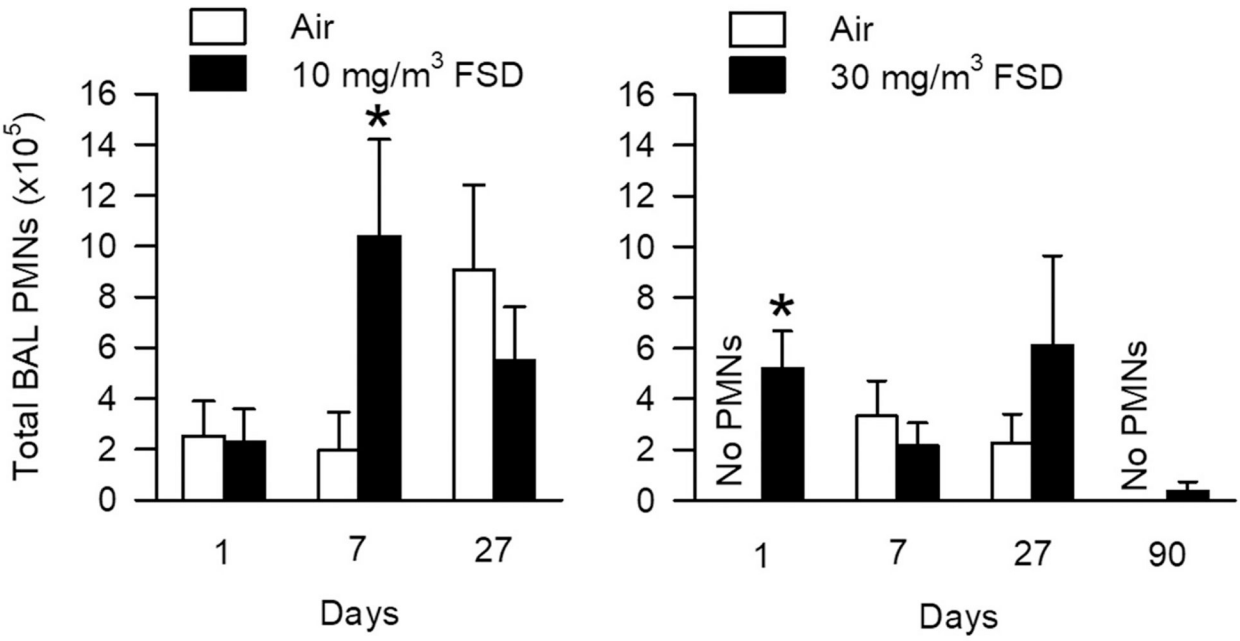

Fig. 5.

Reactive oxidant generation in the BAL cells of rats. Rats were exposed to FSD 8 at 10 or 30 mg/m^3. The chemiluminisence activity was determined as described in the text at post-exposure intervals as indicated in the figure following the exposure.

Author Manuscript Author Manuscript Author Manuscript Author Manuscript

Table 1

BALF cytokines in rats exposed to 10 mg/m^3 FSD 8.

Cytokine	1-day Air	1-day FSD	7-days Air	7-days FSD	27-days Air	27-days FSD
G-CSF	4.19 ± 0.480	5.12 ± 0.460	4.00 ± 0.350	3.84 ± 0.490	3.91 ± 0.710	3.46 ± 0.740 *
DM-CSF	4.04 ± 0.670	4.38 ± 1.05	3.79 ± 0.550	4.25 ± 0.850	4.20 ± 0.480	4.94 ± 0.660
EGF	1.43 ± 0.270	1.51 ± 0.180	1.11 ± 0.300	1.23 ± 0.100	1.55 ± 0.250	2.06 ± 0.430
GRO/KC	147 ± 9.35	145 ± 9.13	156 ± 8.22	187 ± 19.6	187 ± 26.9	173 ± 16.7
VEGF	1160 ± 129	908 ± 60.4	1010 ± 135	1160 ± 138	1880 ± 188	1180 ± 130
Leptin	96.3 ± 25.6	67.9 ± 15.8	63.5 ± 18.1	62.7 ± 9.50	65.2 ± 12.2	65.8 ± 22.9
CXXL5	66.9 ± 5.12	56.8 ± 3.07	65.2 ± 6.03	96.5 ± 11.5 *	99.9 ± 27.8	65.0 ± 7.17
CX3CL1	36.3 ± 4.10	46.3 ± 3.60 *	33.9 ± 2.33	56.1 ± 3.05 *	49.5 ± 6.21	44.2 ± 3.76
MIP-1α	4.08 ± 0.140	4.97 ± 0.330 *	3.22 ± 0.260	4.66 ± 0.140 *	4.65 ± 0.470	3.83 ± 0.240
MIP-2	43.4 ± 5.45	40.7 ± 3.65	41.6 ± 2.84	49.7 ± 6.56	52.7 ± 8.39	51.6 ± 6.38
MCP-1	271 ± 15.7	273 ± 7.78	267 + 10.47	264 + 10.8	298 ± 13.6	293 ± 12.0
TNF-α	1.36 ± 0.240	1.72 ± 0.360	1.14 ± 0.200	1.57 ± 0.170	1.84 ± 0.240	1.69 ± 0.190
IL-1α	ND	3.26 ± 1.28	3.13 ± 1.78	1.78 ± 0.430	2.69 ± 0.990	ND
IL-β	26.9 ± 1.33	27.7 ± 1.35	24.67 ± 1.36	27.7 ± 1.72	26.3 ± 2.52	24.1 ± 1.97
IL-6	54.5 ± 12.9	39.6 ± 9.78	11.3 ± 2.42	34.0 ± 7.64 *	35.4 ± 10.2	22.1 ± 8.47
IL-2	25.7 ± 1.84	24.0 ± 2.00	19.5 ± 1.47	21.9 ± 1.86	21.2 ± 2.68	20.2 ± 1.87
IL-4	3.14 ± 0.520	5.96 ± 1.69	2.84 ± 0.990	2.28 ± 0.710	5.77 ± 1.73	3.47 ± 0.540
IL-10	9.94 ± 0.980	12.9 ± 1.36	9.20 ± 1.01	10.1 ± 0.920	11.1 ± 1.75	11.2 ± 2.66
IL-12	5.53 ± 0.350	7.73 ± 0.960 *	4.73 ± 0.470	5.81 ± 0.310	7.15 ± 0.620	8.26 ± 0.520
IL-17A	2.46 ± 0.720	1.75 ± 0.400	1.10 ± 0.550	1.59 ± 0.940	1.85 ± 0.790	0.390 ± 0.150
IL-18	355.5 + 17.0	354 ± 18.8	261 ± 19.7	282 ± 18.2	319 ± 22.1	351 ± 34.5
RANTES	1.63 ± 0.110	1.95 ± 0.230	1.44 ± 0.0900	1.60 ± 0.0800	1.47 ± 0.120	1.54 ± 0.0300
IFN-γ	2.62 ± 0.820	10.6 ± 4.61	4.51 ± 1.31	2.73 ± 0.510	2.42 ± 0.610	ND.
IP-10	21.2 ± 2.00	18.5 ± 1.31	16.2 ± 0.920	18.9 ± 1.18 *	29.3 ± 5.48	17.0 ± 1.47
Eotaxin	8.03 ± 0.480	7.57 ± 0.420	7.60 ± 0.420	7.76 ± 0.400	6.95 ± 0.500	7.80 ± 0.450
IL-5	9.26 ± 2.06	9.80 ± 2.78	4.56 ± 2.06	7.87 ± 2.54	7.39 ± 1.85	9.48 ± 3.25
IL-13	ND	1.37 ± 0.600	1.10 ± 0.540	0.76 ± 0.160	1.85 ± 0.650	ND

ND = Not detectable.

* Air vs. FSD, $P < 0.05$.

Author Manuscript Author Manuscript Author Manuscript Author Manuscript

Table 2

BALF cytokines in rats exposed to FSD 8 (30 mg/m^3).

Cytokine	1-day Air	1-day FSD	7-days Air	7-days FSD	27-days Air	27-days FSD
G-CSF	3.39 ± 1.08	2.85 ± 0.830	0.910 ± 0.300	2.67 ± 0.890 *	1.36 ± 0.590	1.95 ± 0.900
DM-CSF	14.3 ± 2.21	14.3 ± 1.90	10.5 ± 1.39	9.59 ± 0.420	10.6 ± 1.54	11.8 ± 1.04
EGF	1.23 ± 0.290	1.16 ± 0.0800	1.37 ± 0.120	1.11 ± 0.100	0.970 ± 0.110	1.59 ± 0.170
GRO/KC	80.1 ± 4.60	83.1 ± 5.34	122 ± 13.2	87.8 ± 5.43 *	99.2 ± 5.73	99.9 ± 6.06
VEGF	806 ± 132	824 ± 229	1040 ± 105	868 ± 86.47	1220 ± 158	1360 ± 178
Leptin	160 ± 25.4	111 ± 17.6	65.2 ± 10.4	109 ± 13.2	76.4 ± 8.02	63.8 ± 9.65
CXXL5	43.3 ± 7.07	48.9 ± 4.43	64.8 ± 6.33	46.7 ± 3.15 *	55.0 ± 5.34	54.9 ± 5.81
CX3CL1	29.8 ± 1.09	38.2 ± 3.20 *	37.2 ± 2.66	36.9 ± 2.40	34.6 ± 2.55	44.9 ± 3.22 *
MIP-1a	4.06 ± 0.350	4.67 ± 0.360	4.43 ± 0.360	4.62 ± 0.200	4.24 ± 0.390	4.76 ± 0.380
MIP-2	28.6 ± 4.46	38.1 ± 2.22	50.6 ± 5.37	27.2 ± 3.56 *	39.6 ± 2.65	39.5 ± 5.51
MCP-1	133 ± 51.6	133 ± 34.7	173.5 ± 22.8	177 ± 28.7	145 ± 36.9	181 ± 21.7
TNF-α	1.79 ± 0.230	1.78 ± 0.160	1.98 ± 0.350	1.89 ± 0.330	1.95 ± 0.160	1.79 ± 0.200
IL-1α	20.7 ± 4.34	18.4 ± 1.52	18.3 ± 1.98	18.0 ± 2.19	19.1 ± 2.31	16.1 ± 1.68
IL-β	9.63 ± 0.830	8.62 ± 1.16	7.95 ± 0.950	7.46 ± 1.15	6.63 ± 0.900	6.46 ± 0.880
IL-18	318 ± 24.1	140 ± 47.2	305 ± 31.9	258 ± 38.5	221 ± 43.7	263 ± 36.5
IL-2	36.9 ± 1.98	31.0 ± 2.86	34.0 ± 0.800	29.7 ± 2.81	30.2 ± 3.18	26.0 ± 2.32
IL-4	6.36 ± 0.490	7.17 ± 1.54	5.58 ± 0.270	7.85 ± 1.10 *	5.46 ± 0.760	65.8 ± 1.02
IL-10	11.2 ± 1.22	12.2 ± 1.47	12.1 ± 1.33	12.6 ± 2.61	12.0 ± 1.24	12.1 ± 1.49
IL-12	11.5 ± 1.50	10.8 ± 1.67	9.78 ± 1.32	1090 ± 1.43	11.5 ± 1.14	13.4 ± 1.10
IL-17A	6.02 ± 0.820	6.23 ± 1.08	5.93 ± 1.12	6.77 ± 1.14	4.26 ± 0.720	5.46 ± 0.800
IL-18	296 ± 15.2	330 ± 30.4	300 ± 15.8	312 ± 32.8	264 ± 24.7	257 ± 14.7
RANTES	1.53 ± 0.180	1.22 ± 0.120	1.01 ± 0.110	1.57 ± 0.170 *	1.12 ± 0.110	1.13 ± 0.130
IFN-γ	9.17 ± 0.620	6.83 ± 0.800 *	7.91 ± 0.850	8.09 ± 0.910	7.66 ± 0.390	8.90 ± 0.680
IP-10	12.2 ± 1.07	13.3 ± 2.45	17.3 ± 6.13	14.6 ± 1.49	15.0 ± 1.50	13.64 ± 0.960
Eotaxin	4.57 ± 0.690	3.79 ± 0.650	3.64 ± 0.410	3.67 ± 0.430	4.18 ± 0.600	4.12 ± 0.300
IL-5	12.6 ± 2.10	8.14 ± 2.43	10.6 ± 1.16	6.28 ± 1.89	9.59 ± 2.47	6.99 ± 2.55
IL-13	12.1 ± 1.56	14.4 ± 0.930	12.1 ± 0.960	10.9 ± 0.990	11.4 ± 1.27	9.08 ± 1.41

* Air vs. FSD 8, $P < 0.05$.

Author Manuscript

Author Manuscript

Author Manuscript

Author Manuscript

Table 3

Statically significant differentially expressed genes detected in the lungs of rats exposed to (10 mg/m^3) at one day post-exposure.

Gene	Fold change	FDR *P* value
Aryl hydrocarbon receptor nuclear translocator like	−1.89	0.0048
Integrin subunit alpha E (Itgae)	−1.69	0.023
Basic helix-loop-helix family member e41(Bhlhe41)	1.83	0.023
Uncharacterized LOC102551236 (LOC102551236)	−3.08	0.023
D-box binding PAR bZIP transcription factor (DbpP)	5.42	0.023
Mucin 1, cell surface associated (Muc1)	1.56	0.043

Author Manuscript

Author Manuscript

Author Manuscript

Author Manuscript

Table 4

Statically significant differentially expressed genes detected in the lungs of rats exposed to FSD 8 (30 mg/m^3) at seven days post-exposure.

Gene	Fold change	FDR *P* value
Titin-like (LOC103691832)	−10.56	0.04
s-rRNA (Rnr1)	−6.19	0.04
Titin (Ttn)	−3.92	0.04
Fibronectin type III domain containing 5 (Fndc5)	−2.90	0.04
LIM domain binding 3 (Ldb3)	−2.33	0.04